



**FACULTY
OF MATHEMATICS
AND PHYSICS**
Charles University

BACHELOR THESIS

Dean Pavlovič

Properties of solar cells based on polymer-silicon junction

Department of Macromolecular Physics

Supervisor of the bachelor thesis: doc. RNDr. Jiří Toušek, CSc.

Study programme: Physics

Specialization: general physics

Prague 2019

I declare that I carried out this bachelor thesis independently, and only with the cited sources, literature and other professional sources.

I understand that my work relates to the rights and obligations under the Act No. 121/2000 Coll., the Copyright Act, as amended, in particular the fact that the Charles University has the right to conclude a license agreement on the use of this work as a school work pursuant to Section 60 paragraph 1 of the Copyright Act.

In..... date.....

signature

Hereby I would like to give many thanks to my supervisor doc. RNDr. Jiří Toušek, CSc. and my consultant doc. RNDr. Jana Toušková, CSc. for their valuable advises, professional approach and everlasting patience. Further, I warmly thank my lab colleague Mgr. Radka Rutsch for creating some of the samples and also for her clear explanations of the procedures.

Title: Properties of solar cells based on polymer-silicon junction

Author: Dean Pavlovič

Department / Institute: Department of Macromolecular Physics

Supervisor of the bachelor thesis: doc. RNDr. Jiří Toušek, CSc, Department of Macromolecular physics

Abstract:

The aim of this work is to study unconventional materials, namely conjugated polymers, as to be used for photovoltaic purposes. Among these polymers are polyaniline, derivative of polyphenylene vinylene and two derivatives of polythiophene. Four different methods are used to study some of the physical quantities of the samples, that should affect overall efficiency of solar power conversion. Firstly, I-V characteristics yields fill factor and indicates mechanism of charge transport. Method based on surface photovoltage (SPV) estimates diffusion length of the charge carriers - excitons. Impedance spectroscopy and particular method abbreviated CELIV both measure charge carrier mobility. Outcome of this work are the values of these quantities for some of the samples.

Keywords: organic semiconductors, solar cells, mobility, diffusion length, current-voltage characteristic

Content

Introduction.....	1
1. Theoretical part.....	2
1.1. Semiconductors.....	2
1.2. Chemistry of organic compounds.....	4
1.3. Conjugated polymers.....	6
1.4. Photoconductivity and organic solar cells.....	7
2. Investigated compounds.....	9
3. Experimental methods	10
3.1. I-V characteristics.....	11
Apparatus arrangement.....	12
3.2. Surface photovoltaic effect.....	13
Apparatus arrangement.....	16
3.3. Charge extraction by linearly increasing voltage.....	17
Apparatus arrangement.....	18
3.4. Impedance spectroscopy.....	20
Apparatus arrangement.....	20
4. Results.....	21
4.1. I-V characteristics.....	22
4.2. Surface photovoltaic effect.....	25
4.3. Charge extraction by linearly increasing voltage.....	27
4.4. Impedance spectroscopy.....	29
Conclusion	31
Bibliography.....	32
List of Tables.....	34
List of Abbreviations.....	35

Introduction

Sun provides virtually inexhaustible amount of energy to potentially satisfy the entire population's demands. In addition, harvesting solar energy by photovoltaic devices (i.e. solar cells) is ecologically friendly, compared to other sources. Despite, it is still of negligible contribution to the world electricity production, when compared to fossil energy. One of the explanations possibly lies in the material that photovoltaic devices are based on, namely crystalline silicone. Even though silicon (Si) is the second most abundant element of the Earth's crust (first one being oxygen), particular form of silicon suitable for efficient solar cells operation, monocrystalline silicon, is expensive to manufacture. In addition, crystalline silicon is heavy and fragile. Therefore, in past several decades, effort has been made to come up with different materials to be used as an active layer of photovoltaic devices. For this purpose, organic compounds have been proposed, in particular conjugated polymers. They are inexpensive and easy-to-manipulate-with, lightweight and mechanically flexible. In addition, much lower thickness is generally needed to absorb most of the incident sunlight, compared to conventional solar cell. Potentially they can be transparent for visible light to such a degree, that one might use them as a window glass.

Nonetheless, efficiency of organic photovoltaic devices is few times lower than silicon-based solar cells. Even greater obstacle is their low stability and brief life span - they experience fast photochemical degradation. Life span of most organic solar cells is in order of years, whereas conventional solar cells have mean life span of approximately 25 years.

Despite these shortcomings, we believe it is still worth investigating these organic materials by measuring parameters relevant for photovoltaic purposes. Particularly in this work, electric and photoelectric properties of various solar cells based on conjugated polymers will be measured.

1. Theoretical part

1.1. Semiconductors

In band structure theory, semiconductor is characterized by having highest (most energetic) nonempty band of allowed energies fully occupied, next allowed band is empty and two are separated by nonzero (but smallⁱ) energy interval, called a band gap. Highest occupied band of allowed energies in case of semiconductors is called valence band, lowest (least energetic) unoccupied band is called a conduction band. At sufficient temperatures, some electrons in valence band would attain enough energy to leap into the conduction band, thus would be free to move within the material. This would make semiconductor to some extent conductive, however, it normally takes place at very high temperature. Therefore, it is common to exploit other mechanisms to make such leaps more likely (such as light, as discussed later in this chapter). In addition, a vacancy that is produced in valence band allows neighbouring electron to occupy it, but by leaping there, it creates another vacancy and so on. This effect further contributes to semiconductor's ability to conduct current. It is common to call the vacancy "hole" and treat it as a positively charged quasiparticle with some effective mass.

Inside (not only) semiconductor, electrons and holes move for two general reasons. First one is due to the influence of an electric field, whose magnitude we denote E . Electric field causes charged body (carrier) to accelerate, in direction parallel to the field. Later, we are going to see, that intrinsic electric fields might indeed exist in semiconductors. Mean velocity (or more precisely, speed), that the carrier obtains due to the electric field before colliding, is called drift velocity v and similarly this cause of motion is called drift. Charge carrier mobility μ is then implicitly defined:

$$v = \mu E \tag{1}$$

Second cause of motion inside semiconductors is diffusion. After sufficient time passes, excess concentration of particles is always dissipated unless constrained.^[1] Mean distance that carrier travels (due to diffusion) before recombining with its counterpart is called diffusion length L . It is related to diffusion constant D and mean life-time τ of the corresponding carrier:

$$L = \sqrt{D\tau} \tag{2}$$

ⁱ By "small" we mean smaller than in the case of insulators. In fact, there is no sharp distinction between semiconductors and insulators, other than the value of the band gap.

It is common to introduce additional electrons or holes to the semiconductor in order to increase free carrier concentration (and thus conductivity). Such a semiconductor is said to be of n- or p-type (i.e. n- or p-doped). Interesting phenomenon takes place when n-type and p-type semiconductor come in contact with each other and a semiconductor device is formed. Electrons start to flow from n-side to-p side, and holes in opposite direction. However, electrons (holes) that had left n-side (p-side) of semiconductor, had exposed cations (anions), and thus electric field on the interface of p and n side was created. This field accelerates charge carriers in direction opposite to diffusion flow. After sufficient time had elapsed, diffusion and drift currents equalized and created dynamic equilibrium. That way was created semiconductor device, containing space charge region – SCR, with no carriers present (therefore also called depletion region), and two electrically neutral regions adjacent from both sides. This is the structure of a PN junction diode. It should be emphasized, that in general, a semiconductor device can contain multiple space charged regions as well as multiple neutral regions. In this work, we will only be dealing with semiconductor containing a single space charge region and a single neutral region, the latter will be referred to as the “bulk”. Drift takes place only in a SCR, since only there exist electric fields. In the bulk, diffusion occurs.

When electron-hole pair (sometimes referred collectively as exciton) is created in SCR, it is immediately dissociated by electric field, whenever field forces are greater than mutual attractive force of the electron and hole. When electron-hole pair is created in bulk, it must first diffuse into the SCR in order to be dissociated. Otherwise it recombines, and its energy is converted into thermal or vibrational energy. If we sandwich a semiconductor between two electrodes in such a manner, that carriers travel to opposite electrodes after being dissociated, resulting motion gives rise to the electric current. This is the basic mechanism behind solar cells, where we induce electron-hole pair generation by exposing the sample to the light.

1.2. Chemistry of organic compounds

Organic compound is defined by containing a covalently bound carbon atom within its structure.ⁱ Electronic configuration of carbon in its ground state is ${}_6\text{C}: 1s^2 2s^2 2p_x^1 2p_y^1$. One expects that carbon will be able to provide two of its valence electrons to bind covalently with two atoms. Yet empirically we know, that in most cases carbon binds up to four different atoms.^[2] Simplest example of such behaviour is methane CH_4 . This is explained by assuming one electron from 2s orbital to be promoted into empty $2p_z$ orbital, thus generating excited state of the carbon, with electronic configuration ${}_6\text{C}^*: 1s^2 2s^1 2p_x^1 2p_y^1 2p_z^1$.

Experimental evidence further shows, that all four bonds in methane are equivalent. This is explained by hybridization theory, where four valence electrons of carbon in methane are assumed to occupy so-called hybrid orbitals, which are linear combinations of one s and three p orbitals. This particular case of hybridization is called sp^3 hybridization.

In ethylene (ethene) molecule (Fig. 1), another instance of hybridization occurs, sp^2 hybridization. Carbons in ethylene are mutually bound by double bond, in addition both carbons form two single bonds with hydrogens. Orbitals 2s, $2p_x$ and $2p_y$ hybridize, whereas remaining $2p_z$ orbital remains unchanged. Three electrons in hybrid orbitals make energetically equivalent bonds (called σ bonds), while the electron in $2p_z$ orbital forms a π bond in between the carbons (in other words, double bond between the carbon atoms contains one σ and one π bond). Sterically, σ bonds are formed by head-on overlapping of the original atomic orbitals, whereas a π bond is formed by lateral overlapping above and below the plane of the molecule.

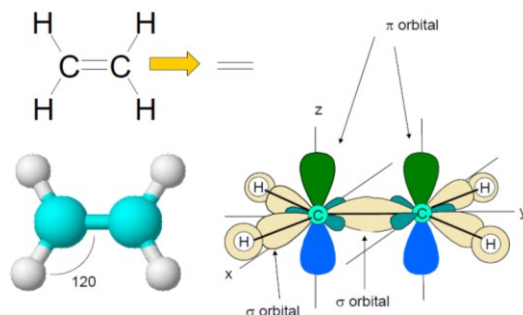


Figure 1 top left: structural formula of ethylene, bottom left: corresponding ball and stick model, right: depiction of molecular orbitals, i.e. bonds [3]

ⁱ There are exceptions to this definition, e.g. carbon dioxide or carbonic acid are not considered organic, despite satisfying conditions of the definition.

Finally, sp^1 hybridization is the case of acetylene (ethyne), where $2s$ and $2p_x$ orbitals hybridize to form two σ bonds, while p_y and p_z orbitals form two π bonds with neighbouring carbon, overall giving rise to triple carbon bond.

1.3. Conjugated polymers

Both carbon excitation and hybridization eventually result in lowering net energy of a molecule, despite the fact that excited carbon C^* has higher energy than ground state carbon C when isolated.

There is another phenomenon which aims to stabilize the molecule, present in conjugated polymers. Conjugated polymers are long chains of carbon atoms with alternating single and double bonds, simplest case being polyacetylene (Fig. 2). In such molecule, electrons of many π bonds delocalize over the entire length (assuming no defects are present) of the carbon backbone, making quasi-continuous energy band equivalent to the valence band of inorganic semiconductor. Similarly, electrons of many π^* antibonding orbitals overlap to create energy band analogous to semiconductors' conduction band. According to [4], we define the band gap as: "the energy difference between the top of the valence band (the highest occupied molecular orbital, or HOMO) and the bottom of the conduction band (the lowest unoccupied molecular orbital, or LUMO)". Quantum mechanics methods can be used to obtain a formula to characterize the band gap.

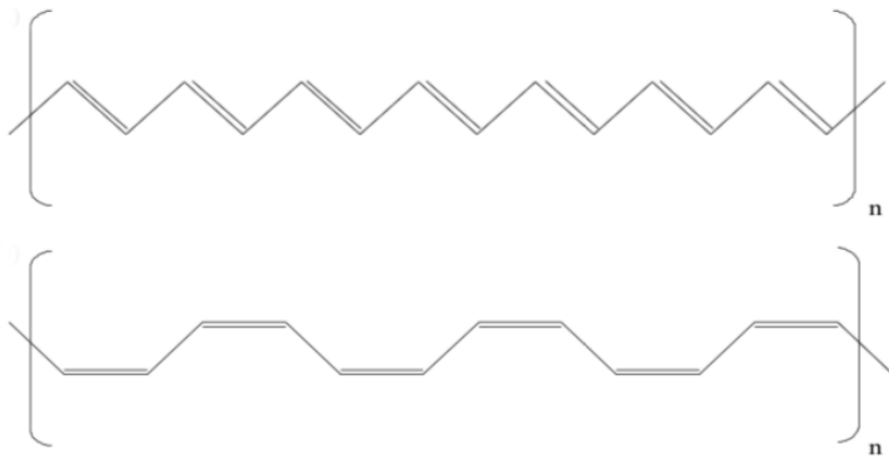


Figure 2 top: *cis*-polyacetylene, bottom: *trans*-polyacetylene [2]

1.4. Photoconductivity and organic solar cells

Just as in case of inorganic semiconductors, electrons from HOMO can be excited into LUMO, leaving behind a hole. One way to do it is by absorbing a photon of sufficient energy, i.e. at least that of a band gap (Fig. 3). Both electron in π^* orbital and hole in π orbital can contribute to the current flow, however, in contrast to inorganic semiconductor, the excited electron is in a bound state with the hole. An energy deficiency, holding them together, is called binding energy. Since they move like a single object, we treat them as a neutral quasiparticle, called exciton.

Now, we see that even though it is common to think of (organic) polymer materials as of insulators, there are some circumstances under which polymers such as polyacetylene become conductive. The mechanism described above is called a photoconductivity. Among the first researchers to discover photoconductivity in organic materials were Alan J. Heeger, Alan MacDiarmid and Hideki Shirakawa. They did so in 1977 on sample of polyacetylene, thus launching a research in the field of conductive polymers.¹ In following years, photovoltaic properties of various organic dyes such as phthalocyanine and chlorophylls were studied. None of the single layer dye solar cells however reached efficiency greater than 0.1%.^[5] In 1982 Weinberger did research on solar cells made of polyacetylene placed between Al and graphite electrodes, measuring open-circuit voltage 0.3 V. This low value is explained by polaron relaxation.^[5] In 1993 Karg et al. investigated Poly(p-phenylene vinylene), i.e. PPV, and its derivatives, which are among most investigated conjugated polymers in the field of photovoltaics.^[5] One example of such derivative is Poly[2-methoxy-5-(2-ethylhexyloxy)-1,4-phenylenevinylene] or MEH-PPV (see Fig 5 in chapter 2). In 1980s, power conversion efficiency as high as 1% was achieved by constructing double layer devices. These two layers create so-called heterojunction, which enhance exciton separation. Electrons readily move to material with higher electron affinity (electron acceptor), and holes to material with lower

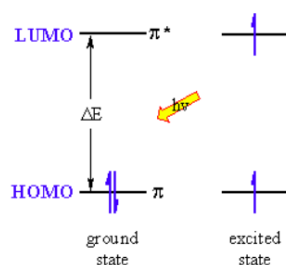


Figure 3 photoexcitation of electron [6]

¹ For their endeavour they were awarded 2000 chemistry Nobel prize.

ionization potential (electron donor).^[5] Most widely used electron acceptor is fullerene C_{60} (Fig. 4) and its derivatives. In 1996 Halls et al. studied PPV/ C_{60} heterojunction solar cells and found diffusion length in order of nanometres. It is a challenge to find optimal material thickness. On one hand, higher the thickness, greater amount of light is absorbed, but carriers might not be able to reach electrodes prior to recombining. On the other hand, small material thickness might mean that majority of light is propagated through the material without absorption. This challenge is overcome by proposing dispersed (bulk) heterojunction solar cells. In this arrangement, donor and acceptor materials are blended together, creating many depletion regions randomly dispersed inside material. Domain sizes of order of diffusion lengths can be achieved. First blend of two different organic dyes was studied in 1991 by Hiramoto.

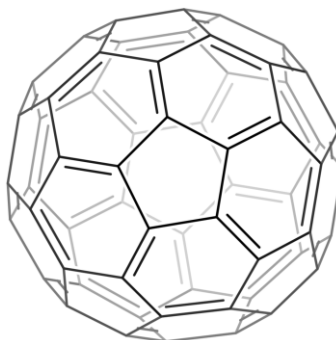


Figure 4 structure of fullerene [7]

2. Investigated compounds

Out of numerous class of conjugated polymers investigated for photovoltaic usage, we chose four particular compounds, all depicted in Fig. 5.

Simplest one is polyaniline, abbreviated as “PANP”. Its repeating unit consist of amino-group attached to a benzene ring, polymerized in 1,4 (i.e. para) position. As will be emphasized in fourth chapter, a chloride salt of polyaniline was used.

Second polymer one already mentioned in previous chapter, namely poly[2-methoxy-5-(2-ethylhexyloxy)-1,4-phenylenevinylene] or MEH-PPV. Its monomeric unit consists of vinylene group on a benzene ring, with two additional oxy-substituents.

Third investigated polymer is called poly(3-hexylthiophene-2,5-diyl), i.e. P3HT. In it, hexyl group is substituted to thiophene ring.

Last one is most complicated, namely poly[[4,8-bis[(2-ethylhexyl)oxy]benzo[1,2-b:4,5-b']dithiophene-2,6-diyl][3-fluoro-2-[(2-ethylhexyl)carbonyl]thieno[3,4-b]thiophenediyl]], abbreviated PTB7.

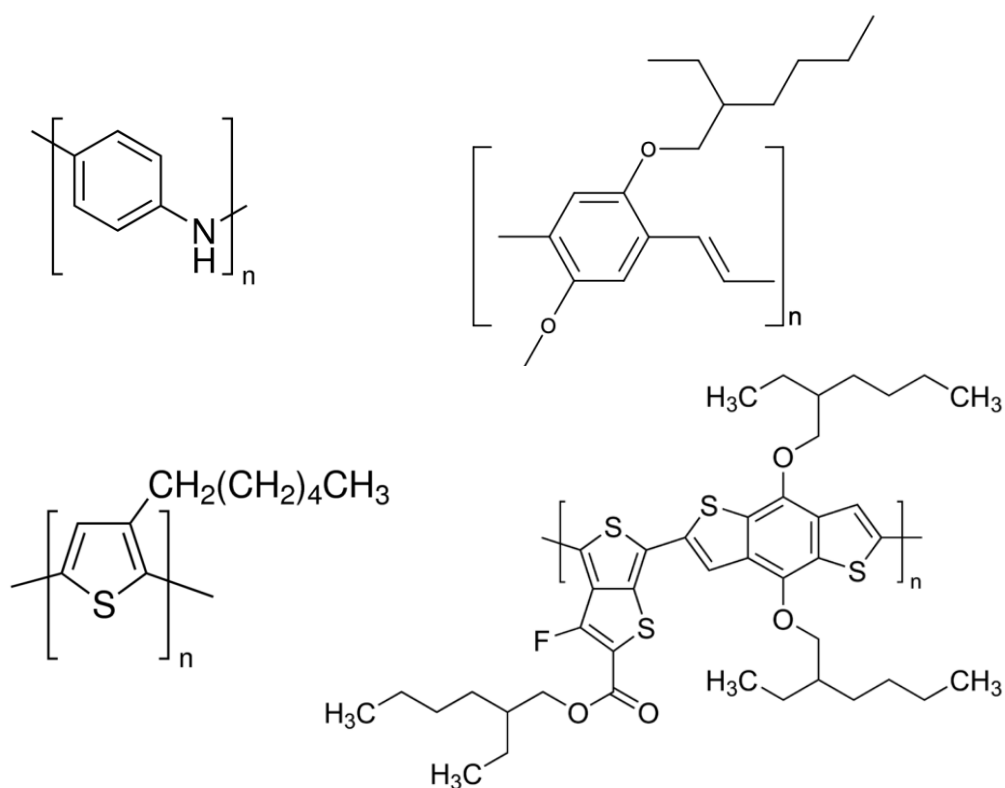


Figure 5 structures of investigated compounds; top left: PANI [8], top right: MEH-PPV [9], bottom left: P3HT [10], bottom right: PTB7 [11]

3. Experimental methods

In this work we are concerned with measuring some of the quantities that are expected to influence efficiency of solar cells. By efficiency, we naturally mean power conversion efficiency (sometimes abbreviated PCE) η defined as the ratio:

$$\eta = \frac{\textit{extracted electrical power}}{\textit{incident light power}}$$

Physical quantitiesⁱ that usually have positive effect on η introduced so far are carrier mobility μ , and diffusion length L . We will further mention open-circuit voltage U_{open} , short-circuit current density j_{short} , fill factor FF and equivalent shunt resistance R_{sh} . Negative influence on power conversion efficiency will have equivalent series resistance R . This chapter will describe four different methods to measure (not only) these parameters.

ⁱ It should be emphasized, that these quantities are not necessarily independent.

3.1. I-V characteristics

First and the simplest experimental method to characterize organic solar cell is to measure a response of electric current density j when subjected to external voltage U . Plot of j^i as a function of U is commonly called I-V characteristics (or I-V curve). If the sample is illuminated, it is called light characteristics, when light is absent, it is called dark characteristics.

Dark characteristics of our samples could not be modelled using the simple Shockley diode equation which is commonly used for inorganic PN homogeneous junction diodes. The equation had to be modified, to included thermal emission term.^[12]

$$j = j_0 \left[\exp\left(\frac{|e|(U - jR)}{nk_bT}\right) - \exp\left(-\frac{|e|(n - 1)(U - jR)}{nk_bT}\right) \right] + \frac{U - jR}{R_{sh}} \quad (3)$$

By $|e|$ we denote a magnitude of an electronic charge, n is a quality factor, k_b is the Boltzmann constant, T is the absolute temperature, R is the equivalent series of a diode and R_{sh} its shunt resistance, finally j_0 is a saturation current density. Eq. (3) is valid for some heterojunction devices.

In light characteristics, we define short circuit current density j_{short} being equal to current density when voltage is zero. Similarly, open circuit voltage U_{open} is a voltage across the terminals of a device (diode) when current is zero.

Lastly, we define fill factor. Let us imagine a rectangle in I-V diagram, such that one vertex is in the origin and opposite vertex lies on some point of I-V curve in fourth quadrant. Then there exists one particular rectangle whose surface area is largest out of all possible inscribed rectangles. Let us denote horizontal and vertical edge of this particular rectangle U_{pt} and j_{pt} respectively. Fill factor is then defined:

$$FF = \frac{j_{pt} U_{pt}}{j_{short} U_{open}} \quad (4)$$

ⁱ Sometimes, it is more convenient to plot current instead of current density.

APARATUS ARRANGEMENT

The sample in I-V measurements was connected to a voltage source KEITHLEY 230 Programmable Voltage Source, where simultaneously we measured current response using KEITHLEY 617 Programmable Electrometer. We recorded current values at pre-defined voltage steps using a computer with ad hoc program. In case of a light characteristics, the sample was illuminated by a 150-Watt halogen lamp with tungsten filament.

3.2. Surface photovoltaic effect

We have seen before, that the two primary causes of motion exist, namely drift and diffusion. We expect the net photogenerated current (density) j_{ph} to be the sum of drift current (i.e. SCR current) and diffusion current (i.e. bulk current), assuming there are no mutual influences of the two^[13], that is:

$$j_{ph} = j_{drift} + j_{dif} \quad (5)$$

In order to extract power from the bulk, excitons must be able to reach SCR before they recombine. We have formerly introduced diffusion length L , as a mean distance that the carrier (in our case exciton) travels prior to recombining. It implies, that higher the diffusion length, greater the chance of exciton reaching SCR and therefore higher the efficiency η of solar cells.

We shall now describe the modified method of measuring diffusion length of a semiconductor based on the surface photovoltaic effect. It was developed in our institute, namely Department of Macromolecular Physics, by J. Toušek and J. Toušková.^[14]

It turns out, that free semiconductor surface often spontaneously creates depletion region. Excess states localized at the surface arise, therefore, it is natural to expect deviation in the electronic concentration. This deviation in carrier density is characterized by bending of the conduction and valence bands in energy diagram. Result is nonzero surface potential and therefore an electric field.

Figure 6 displays our sample and a choice of coordinate system. Sample consists of a p-type semiconductor layer deposited on top of a glass slide coated with indium tin oxide (abbreviated ITO) from adjacent side. This ITO layer shall serve as one of our electrodes. On top of the sample was placed thin insulating Mylar sheet, on top of which was another ITO-coated glass, with ITO surface facing the Mylar sheet (and therefore also the sample). This arrangement forms capacitive coupling. The two ITO layers serve the role of electrodes of parallel plate capacitor and the semiconductor (along with Mylar sheet) serves as the dielectric. We assume that space charge region on one surface of the semiconductor emerged, rest is bulk. As depicted in Fig. 6, we assume now that the bulk is of constant thickness d and is present at the side adjacent to Mylar sheet (this is the case of MEH-PPV sample). Let us place origin of our coordinate system here. Thickness of SCR is therefore constant too, and we denote it by w , according to Fig. 6. In this capacitive coupling arrangement, we measure open circuit voltage U_{open} , for which we assume ideal expression:

$$U_{open} = \frac{k_B T}{|e|} \ln \left(1 + \frac{j_{ph}}{j_0} \right) \quad (6)$$

We will illuminate the sample from the bulk side, by regular light flashes. Result will be an alternating current (AC) in semiconductor, which can overcome capacitive coupling, while blocking DC signal. With the knowledge of absorption coefficient α and reflection coefficients of the material, denoted R_1 at $x = 0$ plane, and R_2 at $x = d + w$ plane, it is possible to calculate photogeneration rate $g(x)$ of excitons. Multiple reflections inside the sample were assumed, and interference was neglected. Result is:^[13]

$$g(x) = \alpha[1 - R_1]\Phi_0 \exp(-\alpha x) + \frac{R_2 \exp\left(-2\alpha \left[w + d - \frac{x}{2}\right]\right)}{1 - R_1 R_2 \exp(-2\alpha[w + d])} \quad (7)$$

where Φ_0 is the incident photon flux density. It is now possible to calculate j_{drift} . Drift current is coming from space charge region and can be calculated by integrating Eq. (7) over the entire SCR, with weighting factor $G(x)$. For simplicity, we assume $G(x) = G$ or that it is constant over the entire space charge region, so it is put before the integral.

$$j_{drift} = |e|G \int_d^{d+w} g(x) dx \quad (8)$$

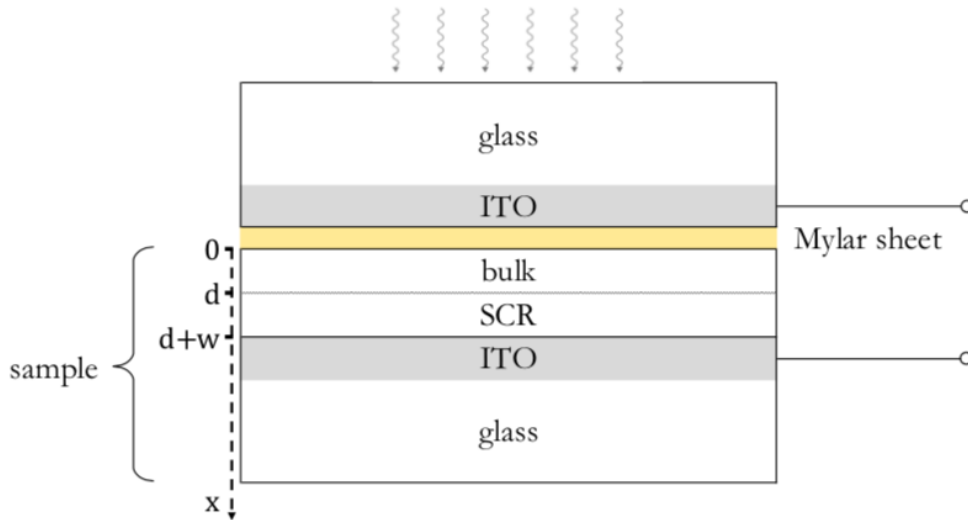


Figure 6 sample arrangement for measuring diffusion length, voltage is measured across two terminals depicted by empty circles

Since there are no fields present in the bulk, we can calculate contribution from the bulk by solving the diffusion equation. We denote exciton concentration $c(x)$ as a function of position inside semiconductor. Diffusion equation has the form:

$$\frac{d^2c(x)}{dx^2} - \frac{c(x)}{L} = -\frac{g(x)}{D} \quad (9)$$

It is a second order ordinary differential equation, two boundary conditions are required to get a unique solution $c(x)$. Those conditions are:^[13]

$$\begin{aligned} c(d) &= 0 \\ D \frac{dc(x)}{dx} \Big|_{x=0} &= sc(x)|_{x=0} \end{aligned} \quad (10)$$

First condition states, that the exciton concentration vanishes at the interface of SCR and bulk. This comes from assuming perfect sweeping of photocarriers by the SCR.^[13] Second one characterizes recombination at the edge of the semiconductor (adjacent from the bulk side) by some surface recombination velocity s . After solving the equation, we can finally obtain diffusion current density coming from the bulk, by evaluating at the interface of SCR and bulk:

$$j_{dif} = |e|D \frac{dc(x)}{dx} \Big|_{x=d} \quad (11)$$

Solution to (9) evaluated according to (11) is:^[13]

$$\begin{aligned} j_{dif} &= \frac{a_1 \alpha L}{1 - \alpha^2 L^2} \times \left\{ \frac{[\sinh(d/L) + sL/D \cosh(d/L)] \exp(-\alpha d) - \alpha L - sL/D}{sL/D \sinh(d/L) + \cosh(d/L)} + \alpha L \exp(-\alpha d) \right\} \\ &+ \frac{a_2 \exp(-\alpha w) \alpha L}{1 - \alpha^2 L^2} \times \left\{ \frac{\sinh(d/L) + sL/D \cosh(d/L) + (\alpha L - sL/D) \exp(-\alpha d)}{sL/D \sinh(d/L) + \cosh(d/L)} - \alpha L \right\} \end{aligned} \quad (12)$$

Where we abbreviated:

$$\begin{aligned} a_1 &= \frac{|e| \Phi_0 (1 - R_1)}{1 - R_1 R_2 \exp(-2\alpha d - 2\alpha w)} \\ a_2 &= \frac{|e| \Phi_0 (1 - R_1) R_2 \exp(-\alpha d - \alpha w)}{1 - R_1 R_2 \exp(-2\alpha d - 2\alpha w)} \end{aligned}$$

We see it depends on L (among other parameters). Therefore, with the knowledge of j_{drift} and using Eq. (5) we can in principle express diffusion length as a function of net photogenerated current. Thus, diffusion length can be estimated.

For complete calculation, we refer to [13].

APPARATUS ARRANGEMENT

Our apparatus for measuring diffusion length is schematically depicted in Fig. 7. Sample in arrangement corresponding to Fig. 6 was placed in holder and illuminated by light source. Light was chopped using optical chopper, which exploits rotating disk to block incident light in periodic intervals. Because the light source emits at broad range of wavelengths, monochromator was used to extract very narrow interval of wavelengths. While the sample was illuminated, voltage was measured using lock-in amplifier, capable of extracting the signal even in very noisy conditions. Measurement was done for broad range of wavelengths, mostly in visible light window. For this purpose, stepper motor was used, which varies wavelength extracted by monochromator.

According to [15], photogenerated current density j_{ph} is usually much smaller than saturation current density j_0 , allowing us to expand logarithmic function in Eq. (6) and conclude, that photogenerated current are linearly proportional, or that $j_{ph} \propto U_{open}$. We therefore measure voltage instead of current, which is much more convenient.

Outcome of the experiment was data table with measured photovoltage (which is in fact open circuit voltage U_{open}) as a function of wavelength λ . This data was put into program, which contained algorithm based on theory discussed earlier in this chapter, capable of fitting measured data into the theoretical model. Program required the knowledge of absorption coefficient α and reflection coefficients R_1 and R_2 of the material. Prior to the experiment, we were given the intensity spectrum of used light source and the spectra of absorbance and reflectance yielding these parameters. Fitting was done mostly manually, by observing and minimizing sum of the least squares. Main outcome of the program was the diffusion length L , bulk thickness d and the space charge region thickness w . We also obtained values of surface recombination velocity s and weighing factor G of integral in Eq. (8) called gain, but we do not consider them important in this work and therefore omit their values.

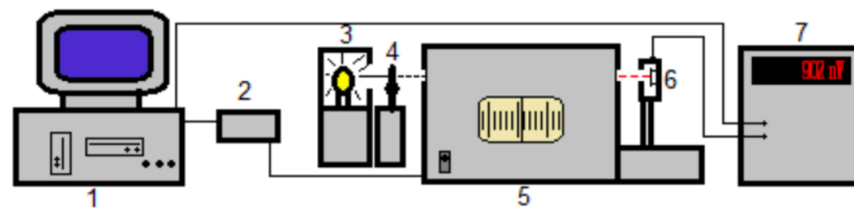


Figure 7 apparatus arrangement for measuring diffusion length: 1. computer, 2. stepper motor, 3. light bulb, 4. optical chopper, 5. monochromator, 6. sample, 7. lock-in amplifier [16]

3.3. Charge extraction by linearly increasing voltage

Mobility of charge carriers μ defined by Eq. (1) is an important physical quantity that characterizes materials used for photovoltaic purposes.

We present a method that can be used to measure μ , introduced by Juška in [17]. The method is called “Charge Extraction by Linearly Increasing Voltage”, abbreviated as “CELIV”. Charge carriers can be photoinduced (generated by light pulses), in such case we call the method “Photo-CELIV”. In our case, we were dealing with p-type materials in equilibrium, where the system had a certain concentration of free charge carriers already in the dark. Therefore, no light pulses were necessary.

Let us imagine a thin layer of organic polymer between two electrodes, the blocking electrode on the top. We treat this sample as a parallel plate capacitor with layer of material in between the (dissimilar) capacitor plates. Let us assume triangular (sawtooth) voltage input U , with slope A (see Fig. 8 top for the positive part of signal). The pulse starts at negative value, which corresponds to forward bias of the structure and gradually builds up to positive value – reverse bias. If the material between capacitor plates had been a regular insulator (dielectric), current response would have been square pulse with height $j(0)$, since current of the capacitor is linearly proportional to derivative of voltage with respect to time, which is constant, in our case A .

In case of our samples however, we expect a current response similar to that in Fig. 8 bottom. Explanation is, that in forward bias of the sample, majority charge carriers (holes) are being injected into the sample,^[19] which results in rising the current above the hypothetical dielectric-material case. After the voltage pulse intercepts zero, this injection ceases, and the ongoing reverse bias extract the injected charge, so that the current density

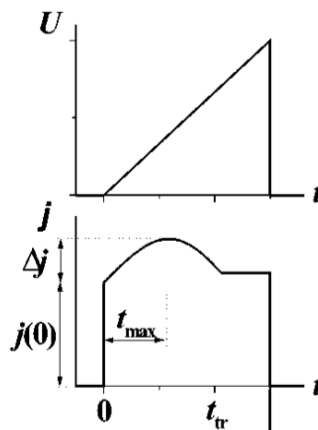


Figure 8 top: positive part of sawtooth voltage pulse applied to the sample during CELIV measurement, bottom: expected current response of the sample [18]

gradually converges back to $j(0)$. We shall call the maximum value of the current $j(0) + \Delta j$. Time elapsed between voltage intercepts zero and current attains its maximum, shall be denoted t_{max} .

In order to compute charge carrier mobility, we are forced to introduce few approximations to our system. Firstly, we require that one charge carrier (holes in our case) is much more mobile than the other. Secondly, we require that the distance between the electrodes (which is equal to the material thickness $d + w$) is negligible compared to the surface area of electrodes. This is the parallel plate capacitor approximation. For third, we assume moderate conductivity of sample, which is equivalent to Δj being same order of magnitude as $j(0)$. As a consequence, we can use a simple formula for computing the mobility of charge carriers.^[18]

$$\mu = \frac{2}{3} \frac{(d + w)^2}{At_{max}^2 \left(1 + 0.36 \frac{\Delta j}{j(0)}\right)} \quad (13)$$

APPARATUS ARRANGEMENT

A thin layer of organic polymer was placed on a substrate, coated with conductive material, serving as the bottom electrode. On top of the sample was formerly evaporated another electrode, so that a diode-like device was formed. In Fig. 9 we display PANI/Si sample, where top electrode is made of gold and bottom electrode is made of indium. Bottom electrode is located under the silicon (so that it is not in direct contact with polymer). Because of this dissimilarity, there exists a difference in work functions between the top and the bottom electrode. When external voltage U is applied to the sample, the difference in work functions has to be taken into account and added to or subtracted from the source voltage.

Circuit for CELIV measurement was relatively simple, see Fig. 9. Between the electrodes was brought time-dependent voltage from generator Agilent 3210A. In series with the sample was placed oscilloscope OWON SmartDS 7102V with internal 50Ω resistance. Oscilloscope showed voltage as well as current signal. Parallel to the voltage source was placed another 50Ω resistor. Computer was used to gather data from the oscilloscope, so that relevant parameters t_{max} , Δj and $j(0)$ could be measured.

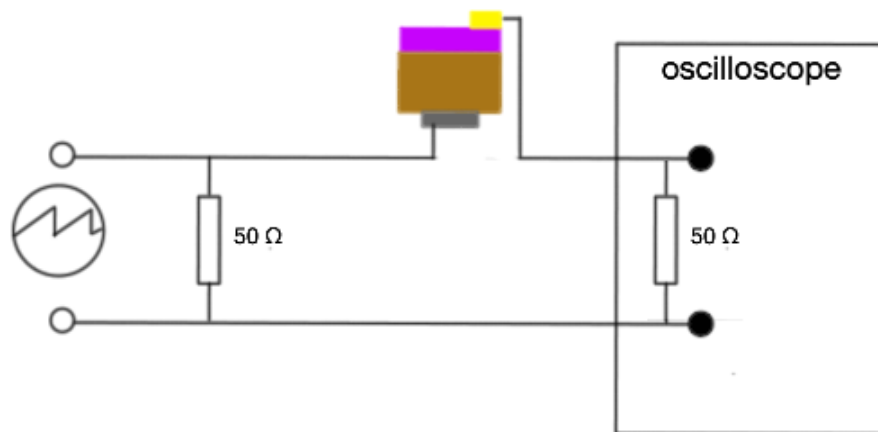


Figure 9 measuring circuitry for CELIV, voltage generator is depicted by a circle with a sawtooth pulse in it; layers of the sample bottom to top: In electrode, n-doped Si, PANI, Au electrode

3.4. Impedance spectroscopy

Second method used to measure charge carrier mobility is impedance spectroscopy.

Impedance Z of a material generalizes the notion of resistance, for purpose of analysing AC circuit responses. It is a complex quantity, whose real part is the resistance, and imaginary part is called a reactance. Impedance in general is frequency-dependent.

In impedance spectroscopy, reactance is studied as a function of AC voltage frequency at constant negative voltage U_{bias} applied to the sample. Reactance spectrum typically consist of one peak, whose maximum shifts horizontally by changing the value of U_{bias} .

With the knowledge of impedance spectrum, we can use formula similar to (13) to calculate the mobility μ of charge carriers. Instead of t_{max} we use reciprocal of frequency value, at which reactance attains its minimum value. Factor 0.44 is added, that has to do with possible dispersion of time of flight according to [19].

$$\mu = \frac{(d + w)^2 f_{max}}{0.44 \times |U_{bias}|} \quad (14)$$

In general, mobility is dependent on the electric field E . By plotting the mobility as a function of the square root of electric field, we can extrapolate to find theoretical value of mobility at zero field, according to Poole-Frenkel theory.^[19] We denote this mobility μ_0 .

APPARATUS ARRANGEMENT

Sample arrangement as well as circuit for impedance spectroscopy was the same as one for CELIV (Fig. 9), except that instead of oscilloscope, an impedance spectrometer (Agilent E4980A Precision LCR Meter) is used, connected to computer. Impedance spectrometer displays magnitude and phase angle of the impedance, which can be transformed into Cartesian coordinates, yielding resistance and reactance. Computer was used to control the measuring parameters, such as U_{bias} and frequency range. AC oscillation level was 100 mV. Examined frequency range was 100 Hz – 2 MHz.

4. Results

Samples with PANI come from Institute of Macromolecular Chemistry, Czech Academy of Sciences. To be precise, chloride salt of polyaniline was investigated. P3HT samples come either from Institute of Physics, Slovak Academy Sciences or from Institute of Macromolecular Chemistry, Czech Academy of Sciences. Both MEH-PPV and PTB7 samples come from Centre of Polymer Systems of Tomáš Bat'a University in Zlín.

Common sample arrangements are depicted in Fig. 10. When no metal electrode is present, ITO layer assumes its role.

All measurements were done at room temperature.

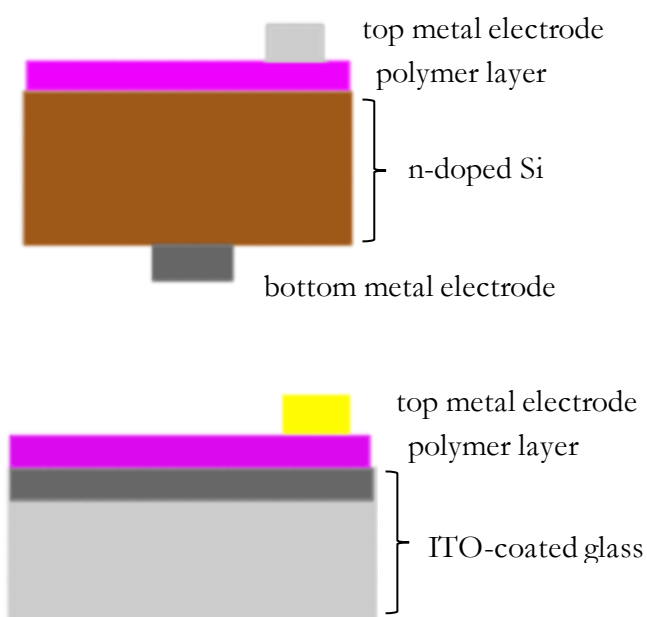


Figure 10 most-used sample arrangements, top: polymer on Si, middle: polymer on ITO

4.1. I-V characteristic

In this subchapter, instead of current density, we will use current I , since sample dimensions were not measured. By I_0 and I_{pt} we denote analogical quantities to j_0 and j_{pt} .

We successfully measured dark characteristics of PANI sample on Si substrate, which comes from 2013. Its arrangement is like in Fig. 10 top. According to model based on Eq. (3) for the dark characteristics we obtained following results:

$$n \doteq 3.0$$

$$I_0 = 6.8 \times 10^{-8} \text{ A}$$

$$R = 138 \ \Omega$$

$$R_{sh} = 1.35 \times 10^5 \ \Omega$$

Plot can be found in Chart 1. By looking at the experimental data, we see almost perfect agreement with theoretical curve. It indicates, that proposed mechanism of charge transport (thermal emission) in PANI/Si heterojunction is verified.

Next, we measured light characteristics of different PANI sample, one which comes from 2019. Sample arrangement is same as in previous one. Its I-V diagram is found in the Chart 2. We obtained following values from the measurement:

$$I_{short} = -7.8 \times 10^{-5} \text{ A}$$

$$U_{open} = 0.18 \text{ V}$$

$$I_{pt} = -4.1 \times 10^{-5} \text{ A}$$

$$U_{pt} = 0.11 \text{ V}$$

$$FF = 32 \%$$

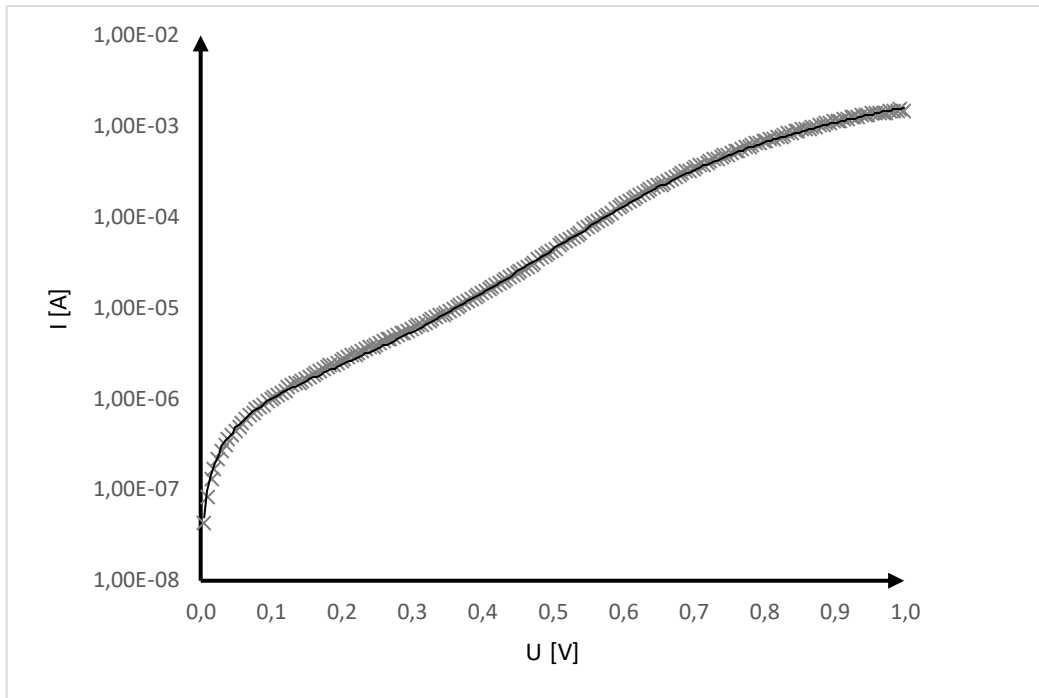


Chart 1 semilogarithmic plot of dark characteristics for 2013 PANI/Si sample, cross marks are experimental data, solid line represents model based on Eq. (3)

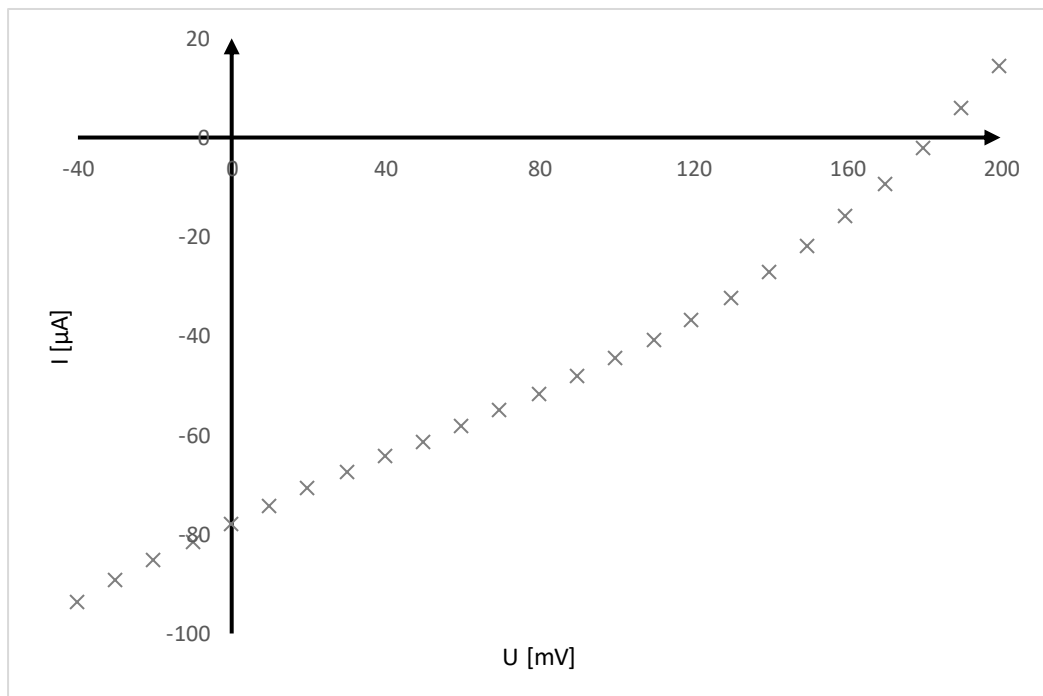


Chart 2 light characteristics of 2019 PANI/Si sample

Lastly, we present light characteristics of PANI on ITO. This sample has a special arrangement, containing layer of titanium dioxide TiO_2 , between the PANI layer and one of the ITO coatings. It is depicted in Fig. 11. ITO coatings served as the electrodes. Experimental data is plotted in Chart 3. From it we obtained following parameters:

$$I_{short} = -1.22 \times 10^{-5} \text{ A}$$

$$U_{open} = 0.29 \text{ V}$$

$$FF = 36.44 \%$$

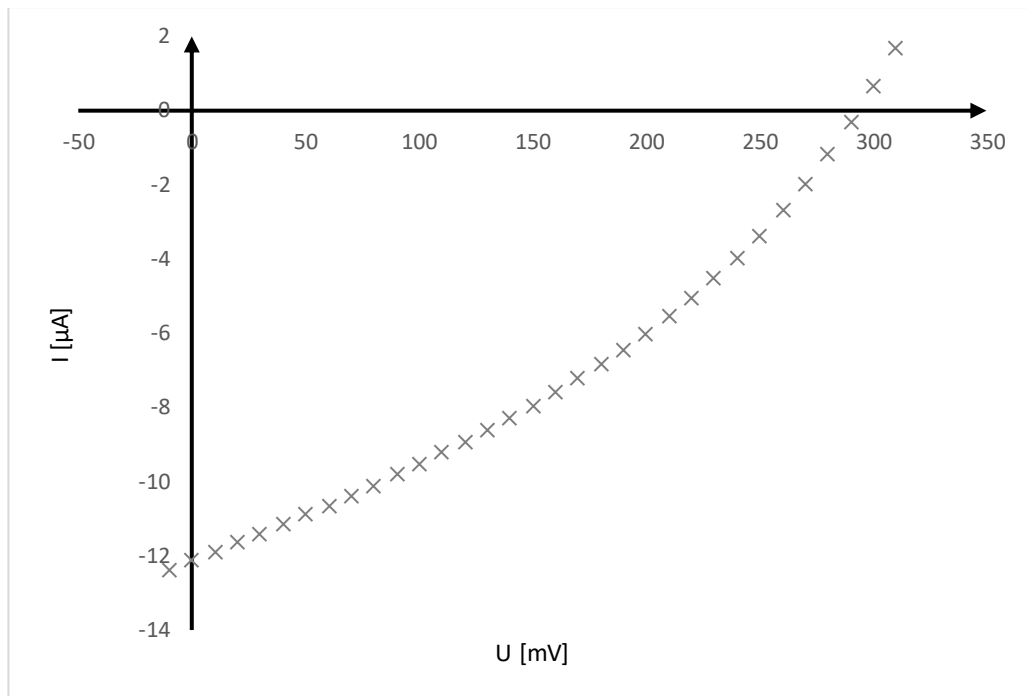


Chart 3 light characteristics of ITO/ TiO_2 /PANI/ITO substrate

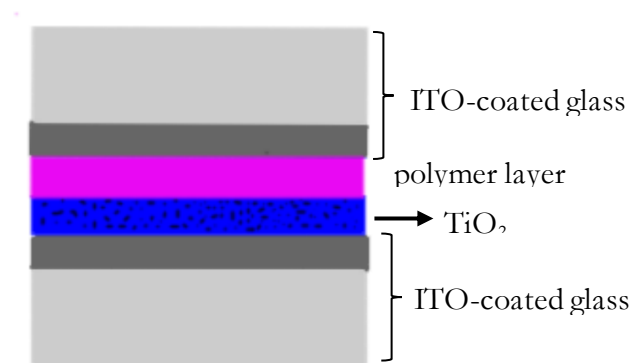


Figure 11 special sample arrangement for I-V measurement

4.2. Surface photovoltaic effect

We successfully measured diffusion length on the sample of PTB7/I^TO. We did so for four different thicknesses. In this case, sample was illuminated through the bulk side, which is adjacent to the surface in direct contact with I^TO.

Next sample was MEH-PPV/I^TO, where bulk is adjacent to the free surface (i.e. surface in contact with Mylar sheet). Therefore, we had to use corresponding light intensity spectrum, taking into account the Mylar sheet in addition to I^TO-coated glass. Results are summarized in Table 1 and two measurements are plotted in Charts 4 and 5.

Table 1 calculated bulk thickness, space charge region thickness and diffusion length

polymer	thickness [nm]	d [nm]	w [nm]	L [nm]
PTB7	50	36	14	11
PTB7	70	34	36	11
PTB7	130	48	82	11
PTB7	230	30	200	16
MEH-PPV	200	29	171	17

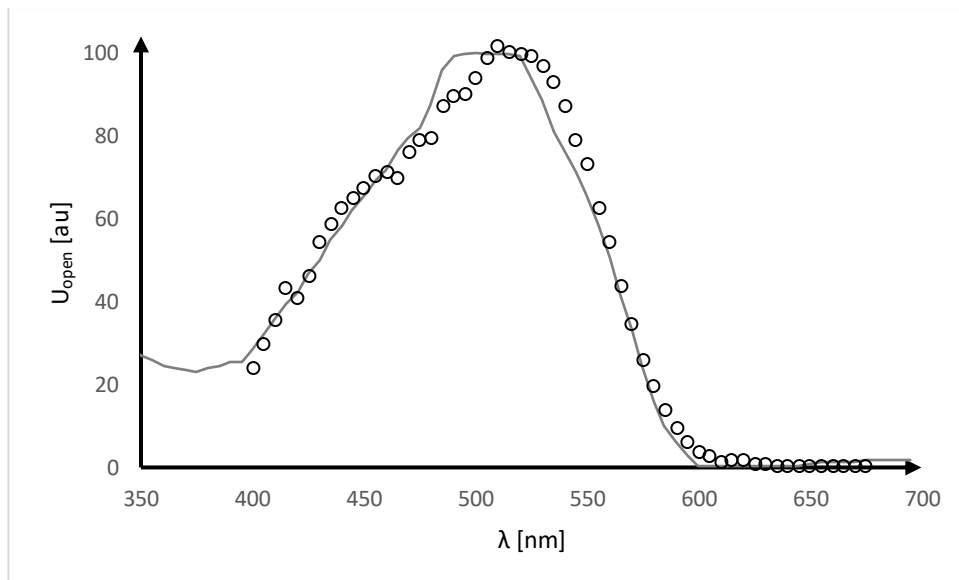


Chart 4 SPV measurement on 200nm MEH-PPV sample, circular marks represent experimental data, solid line represents theoretical curve

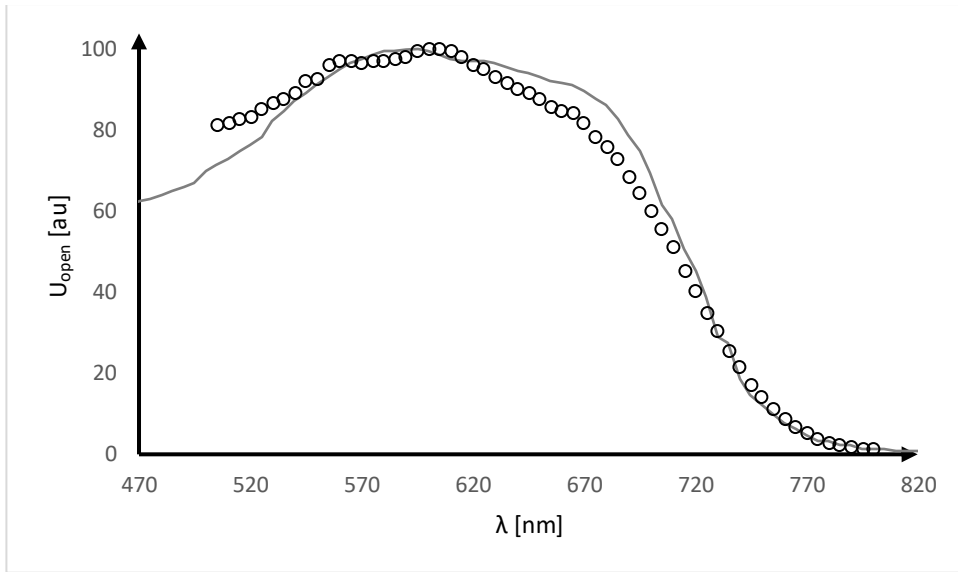


Chart 5 SPV measurement on 130nm PTB7 sample, circular marks represent experimental data, solid line represents theoretical curve

4.3. Charge extraction by linearly increasing voltage

Our samples for CELIV were either P3HT or PANI on either ITO or Si substrate (see Fig. 10). With ITO on glass substrate, no bottom electrode was needed, since ITO layer itself served as an electrode. On the other hand, for samples on silicon, a bottom electrode was deposited. Top and bottom electrodes were always dissimilar (see Table 2). Different voltage amplitudes and periods were applied. In total, seven measurements were successful, all are summarized in Table 2. For most of the calculations, Eq. (13) was further simplified by neglecting the second term in the parentheses of denominator, since current Δj was much smaller than $j(0)$. Two of the measurements are also plotted in Chart 6 and Chart 7.

Table 2 calculated mobility of holes in various samples, based on CELIV method

polymer	thickness [nm]	bottom electrode	top electrode	amplitude [V]	μ [$\text{cm}^2\text{V}^{-1}\text{s}^{-1}$]
P3HT/Si	120	In	Al	3.0	1.00×10^{-5}
P3HT/Si	110	In	Ag	3.0	2.94×10^{-6}
P3HT/ITO	70	-	Al/LiF	5.8	1.88×10^{-6}
P3HT/ITO	70	-	Al/LiF	6.6	3.00×10^{-6}
PANI/Si	160	In	Au	5.0	7.35×10^{-6}
PANI/Si	157	In	Au	6.4	3.89×10^{-6}
PANI/Si	157	Ga	Au	3.3	5.53×10^{-5}

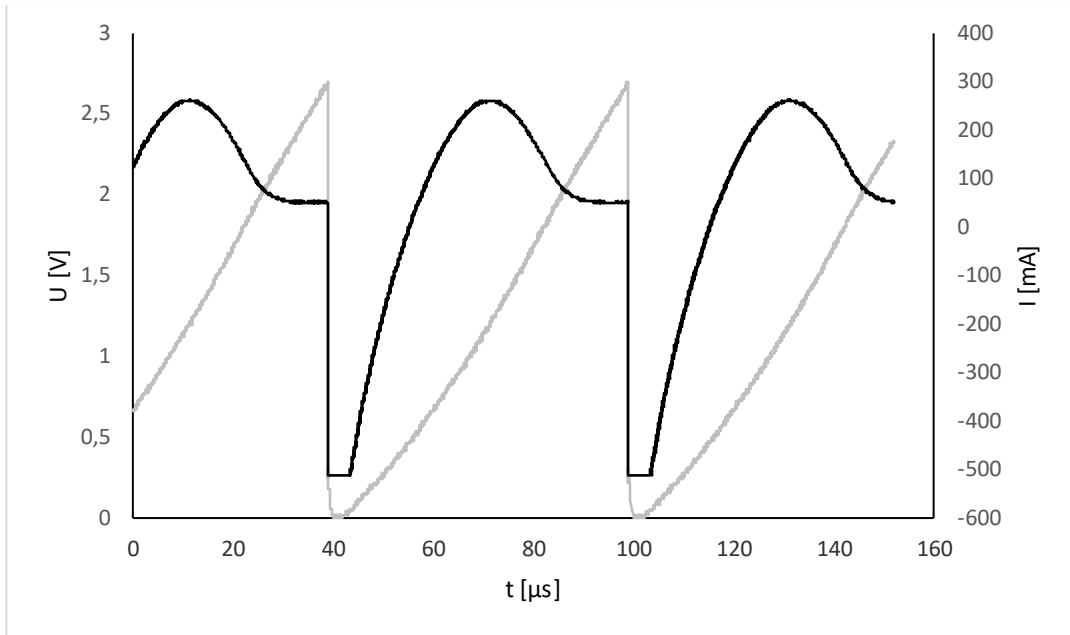


Chart 6 CELIV measurement of 110nm Ag/PH3T/Si/In sample, brighter line represents voltage input, darker line represents current response

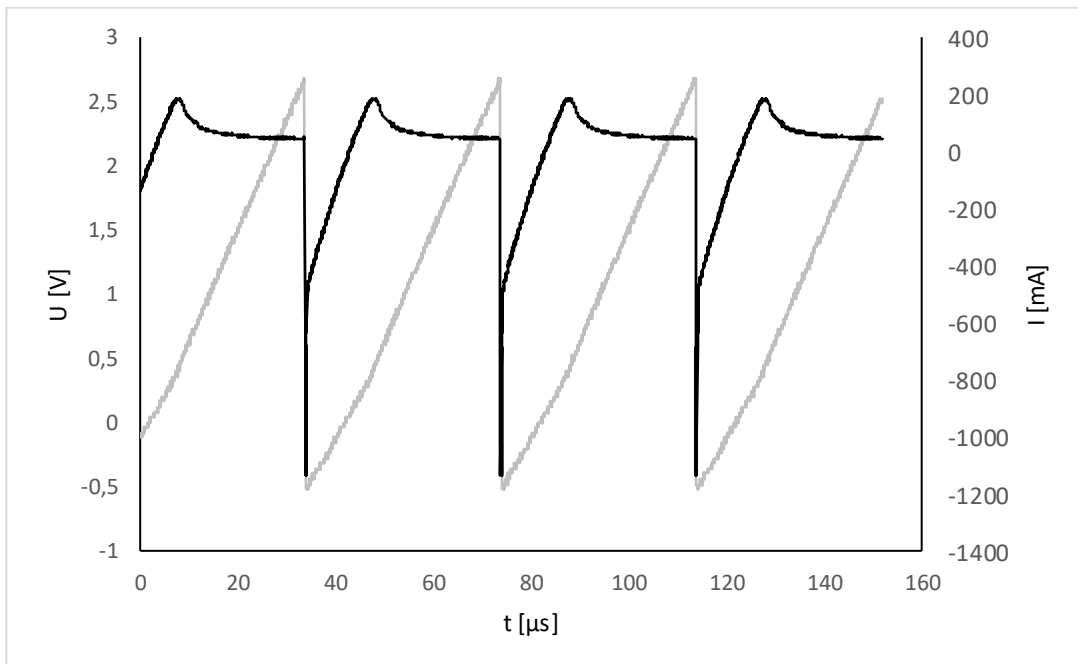


Chart 7 CELIV measurement of 157nm Au/PANI/Si/Ga sample, brighter line represents voltage input, darker line represents current response

4.4. Impedance spectroscopy

In measuring mobility of holes by impedance spectroscopy, we again used Ag/P3HT/Si/In sample. It comes from 2018 and its thickness is 110 nm. We repeated the measurements at values of constant voltage U_{bias} ranging from 0.5 to 3 V. Chart 8 contains normalized spectra of these measurements. In Chart 9 and Table 3 we see mobilities due to Eq. (14) as a function of the square root of electric field. Electric field was simply taken as a voltage U_{bias} divided by the sample thickness. From this we extrapolated Poole-Frenkel mobility:

$$\mu_0 = 1.0 \times 10^{-8} \text{ cm}^2/(\text{V}\cdot\text{s})$$

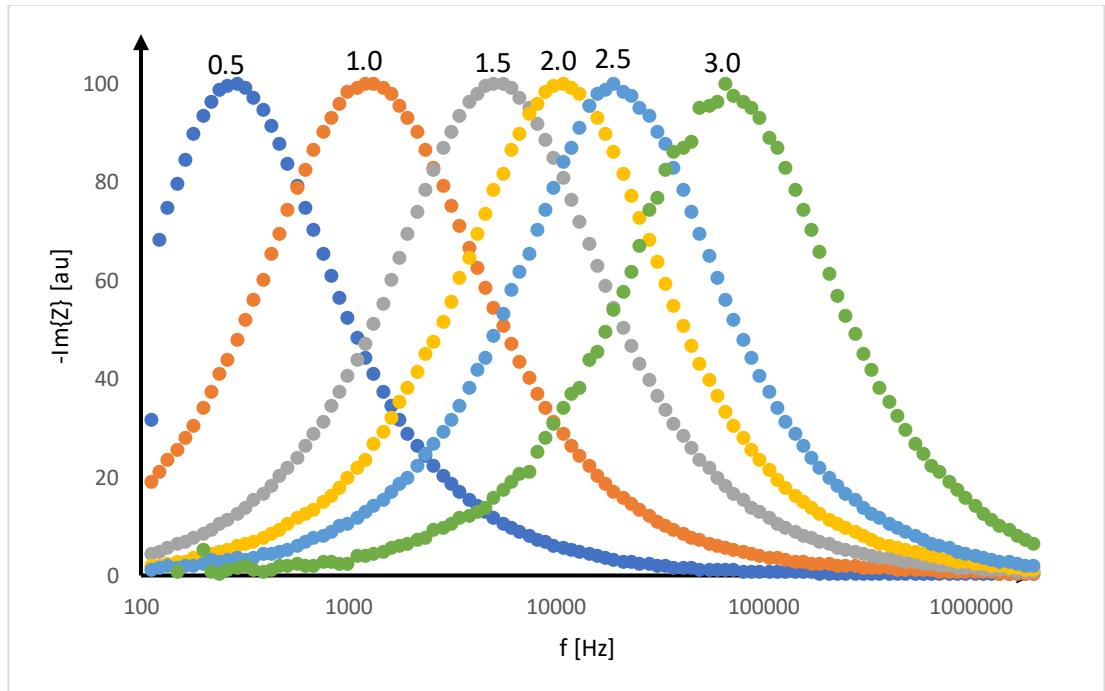


Chart 8 normalized reactance spectra, numbers above the peaks display DC voltage bias

Table 3 mobility of Ag/P3HT/Si/In sample obtained from impedance spectroscopy

U_{bias} [V]	\sqrt{E} [$V^{1/2}cm^{-1/2}$]	f_{max} [Hz]	μ [$cm^2/(V.s)$]
0.5	211.86	288.41	1.61×10^{-7}
1.0	299.63	1204.9	3.36×10^{-7}
1.5	365.46	5536.015	1.04×10^{-6}
2.0	419.61	10789.08	1.53×10^{-6}
2.5	465.83	19110.94	2.20×10^{-6}
3.0	503.83	65979.69	6.50×10^{-6}

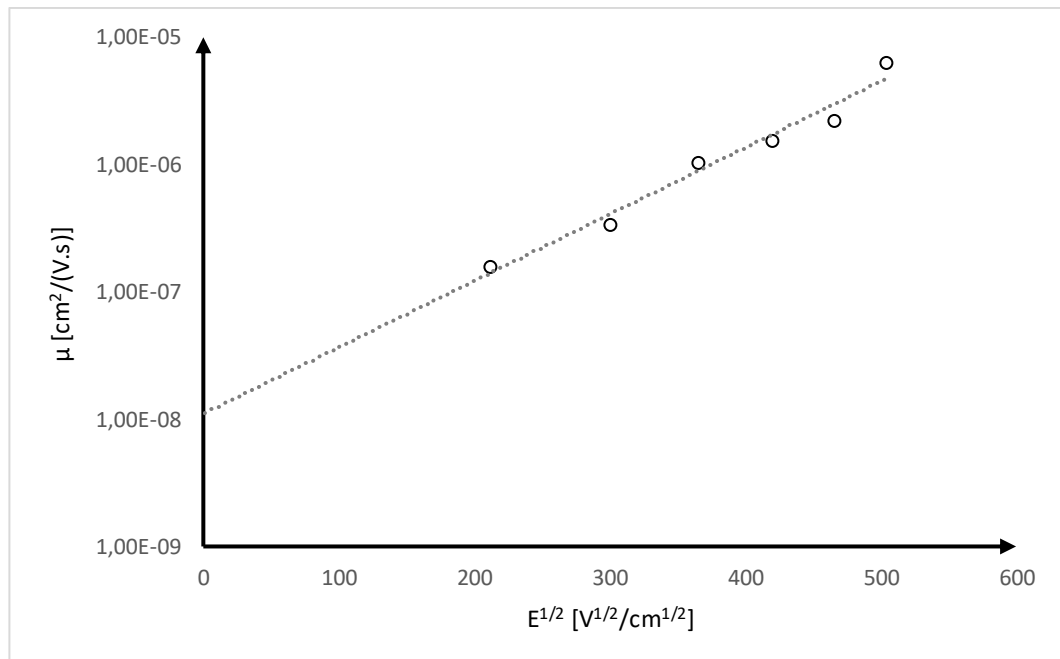


Chart 9 semilogarithmic plot of mobilities obtained from impedance spectroscopy, with Poole-Frenkel mechanism of estimating mobility at zero field

Conclusion

Samples containing one of four different conjugated polymers were investigated in this work. On these samples, four different methods were executed. I-V characteristic was successfully measured on PANI/Si sample, both illuminated and in the darkness. Using Eq. (3) to model dark characteristic turns out to be very accurate, suggesting an emission mechanism of charge transport in the junction. We obtained quality factor $n = 3$. We further got saturation current I_0 , equivalent series and shunt resistance, R and R_{sh} respectively. Light characteristics yielded short circuit current $I_{short} = -7.8 \times 10^{-5}$ A which is quite small, and an open circuit voltage $U_{open} = 0.18$ V. Its fill factor is $FF = 32$ %. Also, we evaluated light characteristics of PANI sample with added TiO₂ layer. From it we got fill factor $FF = 36.44$ %. These low values indicate low efficiency of samples when used as solar cells, according to [1].

SPV measurements were successful on PTB7/ITO and MEH-PPV/ITO. In case of PTB7 four different thicknesses were used, resulting in nondecreasing diffusion length for increasing sample thickness.

CELIV measurement were successfully done on P3HT and PANI samples. In most cases, for each sample, only one particular voltage amplitude produced such current response, that equation (13) could be used. We computed carrier mobilities μ in orders of 10^{-6} to 10^{-5} cm²V⁻¹s⁻¹.

In impedance spectroscopy, only measurements on Ag/P3HT/Si/In yielded expected results. From Chart 8 we can clearly see, how reactance minima (negative of reactance is plotted) are shifting to higher frequencies, with increasing U_{bias} voltage. Values of mobilities are rather low, in order of 10^{-7} to 10^{-6} cm²V⁻¹s⁻¹, with Poole-Frenkel mobility in order of 10^{-8} cm²V⁻¹s⁻¹. Mobility from impedance spectroscopy can be compared to CELIV measurement done on the same sample, which corresponds to 3rd row (including head of the table) in Table 2. Electric field in CELIV measurement is variable, yet we consider value computed from voltage at time equal to t_{max} , according to [20]. Its square root is $\sqrt{E(t_{max})} = 333.03$ V^{1/2}cm^{-1/2}. This value roughly corresponds to the field at $U_{bias} = 1.5$ V from impedance spectroscopy, which is 365.46 V^{1/2}cm^{-1/2}. Thus, we compare values of the mobility from CELIV and impedance spectroscopy. One from CELIV is $\mu = 2.94 \times 10^{-6}$ whereas the other is $\mu = 1.04 \times 10^{-6}$. At the very least, values are at the same order of magnitude.

Bibliography

- [1] GREEN, Martin A. *Solar cells: operating principles, technology, and system applications*. Englewood Cliffs, NJ: Prentice-Hall, c1982. ISBN 01-382-2270-3.
- [2] STELLA, Marco. *Study of Organic Semiconductors for Device Applications*. Barcelona, 2006. Dissertation. Universitat de Barcelona.
- [3] 2005 lecture of René Janssen on “Organic and polymer solar cells” at Eindhoven University of Technology.
- [4] ARCHER, Mary D. a R. HILL. *Clean electricity from photovoltaics*. London: Imperial College Press, c2001. ISBN 978-1-86094-161-0.
- [5] SPANGGAARD H. and KREBS Frederik C. A brief history of the development of organic and polymeric photovoltaics. *Solar Energy Materials and Solar Cells*. 2004, **83**, 125-146. DOI: 10.1016/j.solmat.2004.02.021. ISSN 0927-0248.
- [6] <<http://www.chem.ucalgary.ca/courses/350/Carey5th/Ch13/ch13-uvvis.html>> (cit. 8. 3. 2019)
- [7] <http://www.wikiwand.com/en/Fullerene_chemistry> (cit. 11.3.2019)
- [8] <<https://www.sigmaaldrich.com/catalog/product/aldrich/556459>> (cit. 9. 4. 2019)
- [9] <https://www.researchgate.net/figure/Chemical-structure-of-MEH-PPV_fig2_235126442> (cit. 9. 4. 2019)
- [10] <<https://www.sigmaaldrich.com/catalog/product/aldrich/698997>> (cit. 9. 4. 2019)
- [11] <<https://www.sigmaaldrich.com/catalog/product/aldrich/772410>> (cit. 9. 4. 2019)
- [12] TOUŠKOVÁ, J., D. KINDL, E. SAMOCHIN, J. TOUŠEK, E. HULICIUS, J. PANGRÁC, T. ŠIMEČEK a Z. VÝBORNÝ. Charge transport study and spectral response of GaSb/GaAs heterojunctions prepared by MOVPE. *Solar Energy Materials and Solar Cells*. 2003, **76**, 135-145. ISSN 0927-0248.
- [13] TOUŠEK, J. and J. TOUŠKOVÁ. The role of the space charge region in surface photovoltaic effect. *Journal of Applied Physics*. 2014, **116**(8). DOI: 10.1063/1.4893973. ISSN 0021-8979.
- [14] TOUŠEK, J. and J. TOUŠKOVÁ. A novel approach to the surface photovoltage method. *Solar Energy Materials and Solar Cells*. 2008, **92**(9), 1020-1024. DOI: 10.1016/j.solmat.2008.02.033. ISSN 09270248.

- [15] TOUŠEK, J., J. TOUŠKOVÁ, R. CHOMUTOVÁ, B. PARUZEL a J. PFLEGER. Direct measurement of exciton dissociation energy in polymers. *AIP Advances*. 2017, **7**(1). DOI: 10.1063/1.4975224. ISSN 2158-3226.
- [16] PEČEŇA, Rastislav. *Výzkum organických vrstev pro sluneční články*. Praha, 2011. Bachelor's thesis. Charles University.
- [17] JUŠKA, G., K. ARLAUSKAS, M. VILIŪNAS a J. KOČKA. Extraction current transients: New Method of Study of Charge Transport in Microcrystalline Silicon. *Physical Review Letters*. 2000, **84**(21), 4946-4949. ISSN 0031-9007.
- [18] PIVRIKAS, A., N. S. SARICIFTCI, G. JUŠKA a R. ÖSTERBACKA. A review of charge transport and recombination in polymer/fullerene organic solar cells. *Progress in Photovoltaics: Research and Applications*. 2007, **15**(8), 677-696. DOI: 10.1002/pip.791. ISSN 10627995.
- [19] TOUŠEK, J., J. TOUŠKOVÁ, R. CHOMUTOVÁ, I. KŘIVKA, M. HAJNÁ a J. STEJSKAL. Mobility of holes and polarons in polyaniline films assessed by frequency-dependent impedance and charge extraction by linearly increasing voltage. *Synthetic Metals*. 2017, **234**, 161-165. DOI: 10.1016/j.synthmet.2017.10.015. ISSN 03796779.
- [20] JUŠKA, G., K. ARLAUSKAS, M. VILIŪNAS, K. GENEVIČIUS, R. ÖSTERBACKA a H. STUBB. Transport in π -conjugated polymers from extraction current transients. *Physical Review B*. 2000, **62**(24). ISSN 0163-1829.

List of Tables

Table 1 calculated bulk thickness, space charge region thickness and diffusion length

Table 2 calculated mobility of holes in various samples, based on CELIV method

Table 3 mobility of Ag/P3HT/Si/In sample obtained from impedance spectroscopy

List of Abbreviations

Ag = silver

Al = aluminium

Au = gold

C = carbon

Ga = gallium

In = indium

Li = lithium

Si = silicon

C₆₀ = fullerene

ITO = indium tin oxide

LiF = lithium fluoride

TiO₂ = titanium dioxide

PANI = polyaniline

MEH-PPV = poly[2-methoxy-5-(2-ethylhexyloxy)-1,4-phenylenevinylene]

P3HT = poly(3-hexylthiophene-2,5-diyl)

PTB7 = poly[[4,8-bis[(2-ethylhexyl)oxy]benzo[1,2-b:4,5-b']dithiophene-2,6-diyl][3-fluoro-2-[(2-ethylhexyl)carbonyl]thieno[3,4-b]thiophenediyl]]

HOMO = highest occupied molecular orbital

LUMO = lowest unoccupied molecular orbital

SCR = space charge region

SPV = surface photovoltage

CELIV = charge extraction by linearly increasing voltage

PCE = power conversion efficiency

au = arbitrary units